Tecqnical Paper

大 韓 造 船 學 會 誌
第18卷 第2號 1981年 6月
Journal of the Society of
Naval Architects of Korea
Vol. 18, No. 2, June 1981

A Prediction Method for Three-Dimensional Boundary Layers on Ship Forms at Zero Froude Number

by

Shin-Hyoung Kang*

Abstract

A method to predict the three-dimensional turbulent boundary layer on ship forms is introduced. The present differential method is in the scope of thin boundary layer theory and adopting the eddy-viscosity turbulence model. Two different numerical schemes are taken in this paper to handle the sign-changing cross-flows.

The method is applied to predict the boundary layer development on real ship forms; SSPA Model 720 (C_B=0.675) and HSVA Tanker Model (C_B=0.85). The results are qualitatively in good agreements with measurements except at the very stern. Therefore the method seems to be very promising if further developments are accomplished to handle the thick stern boundary layer effectively.

Nomenclature

A_o	parameter
A^*	van Driest damping factor
A_j, B_j, C_j, D_j	coefficients
C	constant for determining the grid size in y-direction
C_f	local skin friction coefficients
C_p	static pressure coefficients
$F_1(X, Z)$	Y-coordinates of the hull form
$F_2(X, \theta)$	R-coordinates of the hull form
H	shape factor
h_1, h_3, H_3	metric coefficients
K_{13}, K_{31}	geodesic curvatures
k	parameter defined by eq.(21)
L	characteristic length scale
N	parameter
p	static pressure
p^*	parameter
Q, Q_1, Q_2	dependent variables
R_L, R_θ, R_s	Reynolds numbers based on L, θ, s
s	physical distance measured along the stream line direction
T	draft of the ship
U_o	reference velocity
U_1, U_2, U_3	external velocity components in X, Y, Z directions, respectively
U, V, W, W_1, U_s	values of of velocities at the edge of the boundary layer
u, v, w	velocity components in x-, y-, z-directions
u_s, w_s	streamwise and crosswise velocities
u_τ	wall shear velocity

Manuscript received June 13, 1981, Written discussion open until December 15, 1981.

* Member, Ship Research Station, Korea Institute of Machinery and Metals

w_1, w_2	derivatives of w and $\overline{v'w'}$ with respect to z
$-\overline{u'v'}, -\overline{v'w'}$	Reynolds stresses
X, Y, Z	Cartesian coordinate system
X, R, θ	polar coordinate system
x, y, z	orthogonal curvilinear coordinate system
y^*	parameter($=yu_\tau/\nu$)
α	parameter defined by eq.(23)
α	angle of the external stream line
β	cross flow angle
β_ω	limiting cross flow angle
γ	parameter
γ_{tr}	intermittency factor in the transition region
ρ	density of the fluid
τ_w	shear stress at the wall
ε	eddy-viscocity
κ	parameter
δ	boundary layer thickness
δ_1, δ_3	displacement thickness defined by eq. (31)
$\theta_{11}, \theta_{13}, \theta_{31}, \theta_{33}$	momentum thickness defined by eq. (31)
σ, σ_1, π	parameters for turbulence modeling

I. Introduction

The total resistance of a ship in a carm water is devided into the viscous resistance and the residual resistance. It is known that the boundary layer development mainly contribute to the viscous resistance which accounts for as much as 80 to 90 percent of the total resistance in case of cargo ships and oil tankers. As the demand of such full-form ships is increasing with the oil price, energy-saving efforts are more and more important. Therefore the reliable prediction of the boundary layer and wake development will be a critical tool for the hull-form design. Lots of informations about scale effects between the model and the real ship, interactions between the hull and the propeller, and viscous effects on the wave-making resistance can be obtained through the boundary layer and wake calculation. It is well known that the hull form development and the propeller design of good performance in the view point of energy saving cannot be effectively accomplished without comprehensive understanding the flow-fields near the stern.

In spite of the importance of the viscous flow around ship hulls, the application of the three dimensional boundary layer theory to ship forms are far behind that in aeronautics. This is due to the complexity of the ship forms as well as the presence of the free surface. Before the boundary layer calculation, the potential flow field should be obtained from measurements or calculation. This problem is strongly related to theories of wave-making resistance. But it is one of the not-well-developed problems yet. Furthermore highly three-dimensional structures of turbulence developed on the complex geometry is physically unclear yet. Therefore most attempts at the solution of ship boundary layers have been made either with the older integral method or with differential methods based on simple turbulence models during last ten years. These are summarized in the review article by Landweber and Patel [1].

In this paper, studies are restricted to the calculation by the differential method at zero Froude number. The effects of Froude number may be important in case of ships operating at moderate or higher speeds. But the reliable method for calculation of three dimensional boundary layers on the hull at zero Froude number should be developed prior to more general cases. The number of attempts to utilize differential method based on direct numerical solution of the differential equations in ship boundary layer problems are quite less than integral methods. Merits and demerits of the differential and the integral method can-not be easily compared in case of highly three dimensional boundary layer on the ship form. But it is true that more valuable local information may be obtained from the differential method.

Cebeci et al. [2] and Chang & Patel [3] are known to be early attempts to apply the differential method to the fully three dimensional turbulent boundary layer on the ship form [1]. Both employ the isotropic

eddy-viscosity assumption but differ in their numerics and range of application. Cebeci & Chang [4] and Soejima & Yamazaki [5] are continuous works of Cebeci group. Cebeci, Chang and Kaups [6] used a curvilinear non-orthogonal coordinate system to handle the complex geometry and more advanced numerical schemes. Hoekstra [7] calculated the boundary layer development around the bulbous bow at zero Froude number with three different numerical schemes according to the flow conditions. Raven [8] computed the stern boundary layer, whose method is nearly the same as Chang & Patel [3] and Hoekstra [7], but with two-equation turbulence model at the outer region of the boundary layer and a mixing length model very close to the wall. Abdelmeguid et al. [9] and Muraoka [10] employed the non-orthogonal polar coordinate system and the two-equation turbulence model. As discribed above, many researches have been made to develope the general differential method for the boundary layer calculation on ship form. Most of the method show reliable predictions of the turbulent boundary layer development on the ship form except near the stern, where curvatures of the hull-surface are considerably changing and the behavior of the boundary layer is quite different from the so called thin boundary layer. Furthermore reliable flow measurements are not enough to check each method. SSPA-ITTC Ship Boundary Layer Workshop was held in June 1980. That was organized by ITTC and SSPA to compare calculated results each other with given ship forms, initial conditions, and experimental data. Two models were adopted. One is SSPA Model No. 720 ($L/B=7.06$, $B/T=2.40$, $C_B=0.675$), which was tested in the wind-tunnel by Larrson [11]. The other one was HSVA Tanker model ($L/B=6.6$, $B/T=2.70$, $C_B=0.85$), which was tested in the open type wind tunnel by Hoffmann [12]. Six differential methods were represented among total 15 participants. The results are expected to be published in the 16th ITTC preceedings.

The author has adopted Chang and Patel's method [3] as a first introduction of the 3-dimensional turbulent boundary layer calculation on the ship form to Korean Society of Naval Architects[13]. But their original computer program is quite limited in capability to handle the cross-over type cross-flow of ship boundary layers. Therefore so called the zig-zag numerical scheme is adopted in this paper when the cross flow is reverse to the marching direction, as Hoekstra [7] and Raven [8] did.

II. Basic Equations

2.1 Coordinate System and Geometric Parameters

Two coordinate systems fixed to the ship are introduced to describe the geometry and basic equations (Fig. 1). O-XYZ is a Cartesian coordinate system whose XY-plane is an undisturbed free surface and Z is vertical upward. X axis is directed from the bow to the stern. o-xyz are curvilinear orthogonal coordinate system. xz plane are on the hull surface and y axis is outward normal to the surface.

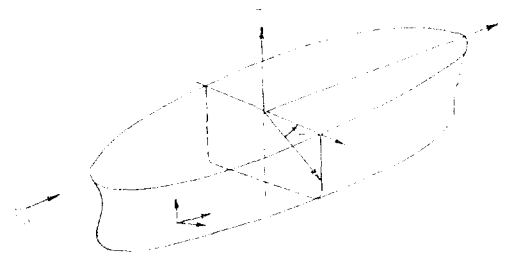

Fig. 1 Coordinate system

The ship is considered to be at rest in the uniform stream of velocity U_o and the ship length is L.

The hull form is described by

$$Y=F_1(X,Z) \tag{1}$$

The above function is used to be given in an offset form. The procedure of the boundary layer analysis is devided into three stages. First, potential flow should be known by calculation or from experiments. Then metric coefficients and geodesic curvatures should be calculated according to the coordinate system adopted. Then the boundary layer will be calculated with boundary conditions and initial conditions according to the region to be calculated. Lots of numerical schemes for the the potential flow are known for accurate and efficient calculations in case of the double

body. Hess and Smith method [14] is most popular among them. Next, the choice of coordinate system for the boundary layer is very important. A non-orthogonal coordinate system is considered to be more capable to handle the complex geometry and the flow. But it still require more extra works. A curvilinear orthogonal system is still popular. Strictly speaking, there exists only one orthogonal coordinate system which may be fixed on the hull surface according to Lame's equations. But it suffices to choose a coordinate system that is orthogonal locally on the hull surface but not necessarily elsewhere. In this case there are a large number of coordinate system. Most popular one is the stream line coordinate system. It is very attractive but the determination of the stream lines and their orthogonal lines requires more efforts. When small cross flow assumptions are applied, it has lots of advantages. But they are dependant on Froude number and also Reynolds number if the displacement effect is taken into account. In this paper, an orthogonal coordinate system is adopted which was proposed by Miloh and Patel [15]. It is dependant only on geometry of the hull.

When we choose $x=X=$constant, that is station line, $z=$constant lines which are orthogonal to the $x=$constant on the hull surface should be determined. In case of a ship with flat bottom XYZ coordinate system is quite limited to describe the hull geometry. A polar coordinates system (X, θ, R) is convenient in such a case. Then the hull surface is given by

$$R=F_2\ (X, \theta) \tag{2}$$

For convenience, we introduce F, T and N such that $F=F_1$, $T=Z$, $N=0$ in a Cartesian coordinate system and $F=F_2$, $T=\theta$, $N=1$ in a polar coordinates system.

Then partial derivatives

$$F_X=\frac{\partial F}{\partial X}$$

$$F_T=\frac{1}{R^N}\ \frac{\partial F}{\partial T}$$

$$F_{XX}=\frac{\partial^2 F}{\partial X^2} \tag{3}$$

$$F_{TT}=\frac{1}{R^{2N}}\ \frac{\partial^2 F}{\partial T^2}$$

$$F_{XT}=\frac{1}{R^N}\ \frac{\partial^2 F}{\partial X \partial T}$$

can be determined by cubic spline functions.

With these derivatives $z=z(X, T)=$constant lines are found by solving the following equation.

$$\frac{\partial T}{\partial X}=-\frac{1}{R^N}\ \frac{F_X F_T}{(1+F_T^2)} \tag{4}$$

The geodesic curvatures are given by

$$K_{13}=\frac{F_X[F_{XT}(1+F_T^2)-F_X F_T F_{TT}+NF_X F_T^3/R]}{(1+F_T^2)^{3/2}(1+F_X^2+F_T^2)} \tag{5}$$

$$K_{31}=\frac{F_X[F_{TT}-N(1+2F_T^2)/R]}{(1+F_T^2)^{3/2}(1+F_X^2+F_T^2)^{1/2}} \tag{6}$$

Let's consider metric coefficients h_1 and h_3 in x and z directions. As will be shown at the next section, the metric coefficient h_3 always occurs in the combination $1/h_3\ \partial/\partial z$ operating on the velocity component. Since x and z are independent variables, we can write

$$\frac{1}{h_3}\ \frac{\partial}{\partial z}=\frac{1}{h_3 z_T}\ \frac{\partial}{\partial T}=\frac{1}{H_3}\ \frac{\partial}{\partial T} \tag{7}$$

Therefore boundary layer calculation can be done with (X, T) coordinate system, once K_{13}, K_{31}, h_1, and H_3 are calculated as follows.

$$h_1=[1+F_X^2/(1+F_T^2)]^{1/2} \tag{8}$$

$$H_3=R^N(1+F_T^2)^{1/2} \tag{9}$$

From eq. (4) to eq. (9) were derived by Miloh and Patel [15] and by Hoekstra [7] in case of a polar coordinate system.

2.2 Boundary Layer Equations

Under the thin boundary layer assumptions (refer Nash and Patel [16]) metric coefficient h_2 of y coordinate can be taken as $h_2=1$. Then the three-dimensional boundary-layer equations for an incompressible fluid are as follows.

Continuity equation

$$\frac{1}{h_1}\ \frac{\partial u}{\partial x}+\frac{\partial v}{\partial y}+\frac{1}{h_3}\ \frac{\partial w}{\partial z}+K_{31}u+K_{13}w=0 \tag{10}$$

x-momentum equation

$$\frac{u}{h_1}\ \frac{\partial u}{\partial x}+v\frac{\partial u}{\partial y}+\frac{w}{h_3}\ \frac{\partial u}{\partial z}+(K_{13}u-K_{31}w)w+\frac{1}{h_1}\ \frac{\partial}{\partial x}\left(\frac{p}{\rho}\right)+\frac{\partial}{\partial y}\left(\overline{u'v'}-\nu\frac{\partial u}{\partial y}\right)=0 \tag{11}$$

z-momentum equation

$$\frac{u}{h_1}\frac{\partial w}{\partial x}+v\frac{\partial w}{\partial y}+\frac{w}{h_3}\frac{\partial w}{\partial z}+(K_{31}w-K_{13}u)u+\frac{1}{h_3}\frac{\partial}{\partial z}\left(\frac{p}{\rho}\right)+\frac{\partial}{\partial y}\left(\overline{v'w'}-\nu\frac{\partial w}{\partial y}\right)=0 \tag{12}$$

where K_{13} and K_{31} denote geodesic curvature as described in the previous section and are related with metric coefficients.

$$K_{13}=\frac{1}{h_1h_3}\frac{\partial h_1}{\partial z},\quad K_{31}=\frac{1}{h_1h_3}\frac{\partial h_3}{\partial x} \tag{13}$$

Therefore K_{13} and K_{31} correspond to rates of convergence of x=constant and z=constant lines respectively. The above equation can be used for laminar flows without Reynolds stress terms. $\overline{u'v'}$ and $\overline{v'w'}$. In this case the unknowns (u, v, w) be determined by solving eq. (10), eq. (11) and eq. (12), with pressures provided. On the other hand $\partial p/\partial x$ and $\partial p/\partial z$ may be determined by potential flow velocities as follows.

$$-\frac{1}{h_1}\frac{\partial}{\partial x}\left(\frac{p}{\rho}\right)=\frac{U}{h_1}\frac{\partial U}{\partial x}+\frac{W}{h_3}\frac{\partial U}{\partial z}+(K_{13}U-K_{31}W)W \tag{14}$$

$$-\frac{1}{h_3}\frac{\partial}{\partial z}\left(\frac{p}{\rho}\right)=\frac{U}{h_1}\frac{\partial W}{\partial x}+\frac{W}{h_3}\frac{\partial W}{\partial z}+(K_{31}W-K_{13}U)U \tag{15}$$

when U and W are velocity components on the surface in x-and z-directions, respectively.

For the flow along the plane of symmetry, special treatments are required. Since w, $-\overline{v'w'}$, K_{13} all vanish on the plane of symmetry, z-momentum equation identically vanish. Therefore boundary layer equations are not closed even for laminar flows. Therefore an additional equation is obtaind by differentiating the z-momentum equation with respect to z along the plane of symmetry.

$$\frac{u}{h_1}\frac{\partial w_1}{\partial x}+v\frac{\partial w_1}{\partial y}+w_1^2+K_{31}uw_1-\frac{u^2}{h_3}\frac{\partial K_{13}}{\partial z}+\frac{1}{h_3^2}\frac{\partial^2}{\partial z^2}\left(\frac{p}{\rho}\right)+\frac{\partial}{\partial y}\left(w_2-\nu\frac{\partial w_1}{\partial y}\right)=0 \tag{16}$$

where $w_1=\frac{1}{h_3}\frac{\partial w}{\partial z}$ and $w_2=\frac{1}{h_3}\frac{\partial}{\partial z}\overline{v'w'}$. The second derivative of the pressure can be obtained by the following equation by the same way as eq. (14) and eq. (15).

$$-\frac{1}{h_3^2}\frac{\partial^2}{\partial z^2}\left(\frac{p}{\rho}\right)=\frac{U}{h_1}\frac{\partial W_1}{\partial x}+W_1^2+\left(K_{31}W_1-\frac{1}{h_3}\frac{\partial K_{13}}{\partial z}U\right)U \tag{17}$$

Since all the conventional ship forms are symmetric about their centerplane, the plane of symmetry flow is developed along the keel. On the other hand, the water plane is another plane of symmetry in case of double models. The boundary layer development along a plane of symmetry is very important. The plane of symmetry boundary layer can be solved independently of the adjacent area, since w_1 is not included in eq. (10) and eq. (11). The results of calculated flow in the plane of symmetry are provided as boundary conditions for the complete boundary layer calculations. Therefore a preliminary picture of the complete flow might be imagined form the plane of symmetry flow.

For turbulent flows, it is necessary to make closure-assumptions of the Renolds stresses $-\overline{u'v'}$ and $-\overline{v'w'}$. Several models have been proposed in the past, ie, mean-velocity-field model, mean-turbulent-kinetic-energy model, mean-Reynolds-stress model etc. or one-equation model, two-equation model, and multi equation model.

An eddy-viscosity model which is originated from Cebeci and Smith[17], are adopted here. This model is still one of simple models, and shows reasonable results in many cases. Recently Choi[18] concluded that proper treatment of the three-dimensionality of the flow is much more important than the turbulence models in determining the overall success of the calculation method, through his research of the boundary layer calculation around bodies of revolution at incidence. It is summarized below.

$$-\overline{u'v'}=\varepsilon\frac{\partial u}{\partial y},\quad -\overline{v'w'}=\varepsilon\frac{\partial w}{\partial y} \tag{17}$$

where ε is an isotropic scalar eddy viscosity. The eddy viscosity is defined by two separate formulas.

In the inner region, ε is defened as

$$\varepsilon=l^2\sqrt{\left(\frac{\partial u}{\partial y}\right)^2+\left(\frac{\partial x}{\partial y}\right)^2} \tag{18}$$

where

$$l=ky\left[1-\exp\left(\frac{y^*}{A^*}\right)\right]$$

$$y^*=\frac{yu_\tau}{\nu},\quad A^*=\frac{A_o}{N} \tag{19}$$

$$N=\sqrt{1-11.8p^*},\quad p^*=-\frac{\partial p}{\partial s}\frac{\nu}{\rho u_\tau^3}=\frac{\nu U_s}{u_\tau^3}\frac{\partial U_s}{\partial s}$$

In the outer region, ε is defined by the following formula.

$$\varepsilon=\alpha\left|\int_0^\infty(U_s-\sqrt{u^2+w^2})\,dy\right|\Big/\left[1+5.5\left(\frac{y}{\delta}\right)^6\right] \tag{20}$$

The empirical factors k, A_o and α, which are assumed to be constant at high Reynolds number, but vary at low Reynolds number in the following manner.

$$k=0.40+\frac{0.19}{1+0.49\sigma^2} \tag{21}$$

$$A_o=26.0+\frac{14.0}{1+\sigma^2} \tag{22}$$

$$\alpha=\begin{cases}0.0168 & ,\ R_\delta>6000\\ 0.0168\times\dfrac{1.55}{1+\pi}, & 425<N_\theta<6000\\ [194.8-128.6\ \log R_\theta+30.925(\log R_\theta)^2 & \\ \quad -2.475\ (\log R_\theta)^3]\times10^{-3} & \\ & ,\ R_\theta<425\end{cases} \tag{23}$$

where $R_\delta=\dfrac{\theta_{11}U_s}{\nu},\quad \sigma=R_\theta\times10^{-3}$

and $\pi=0.55\ [1-\exp(-0.243\gamma^{1/2}-0298\gamma)],$

$$\gamma=\frac{R_\theta}{425}-1$$

In the transition region between laminar and turbulent flow, eddy viscosity given above was multiplied by intermittency factor γ_{tr} to take account of transition effects. γ_{tr} is given by Chan and Thyson [19].

$$\gamma_{tr}=1-\exp\left[-\frac{1}{1200}\frac{U_s^3}{\nu^2}R_{s_{tr}}^{-1.34}(s-s_{tr})\int_{s_{tr}}^{s}\frac{t}{U_s}\,dt\right] \tag{24}$$

where $s-s_{tr}$ denotes the transversed distance along the stream line since the transition started. The start of transition is assumed to occur when one of the following conditions is satisfied.

$$R_\delta\geq1.174\left(1+\frac{22400}{R_s}\right)R_s^{0.46} \tag{25}$$

$$R_\theta\geq320 \tag{26}$$

Before being solved, the above boundary layer equations are non-dimensionalized by following non-dimensional variables.

$$\bar{x}=\frac{x}{L},\quad \bar{y}=\frac{y}{L}\sqrt{R_L},\quad \bar{z}=\frac{\bar{z}}{L},$$

$$\bar{u}=\frac{u}{U_o},\quad \bar{v}=\frac{v}{U_o}\sqrt{R_L},\quad \bar{w}=\frac{w}{U_o}, \tag{27}$$

$$\bar{w}_1=\frac{w_1}{U_o}L,\quad \bar{p}=\frac{p}{\rho U_o^2},$$

$$\bar{K}_{13}=LK_{13},\quad \bar{K}_{31}=LK_{31}$$

Here, U_o and L are characteristic velocity and length, and R_L is Reynolds number $(=U_oL/\nu)$.

For references, let us define integral parameters to represent the boundary layer. If u_s is stream wise velocity component and w_s is cross-wise velocity, then

$$u_s=u\cos\alpha+w\sin\alpha \tag{28}$$

$$w_s=-u\sin\alpha+w\cos\alpha \tag{29}$$

where α denotes external stream line angle and is obtained by

$$\tan\alpha=\frac{W}{U} \tag{30}$$

Then integral parameters are defined as follows:

$$\delta_1=\int_0^\infty\left(1-\frac{u_s}{U_s}\right)dy$$

$$\delta_3=\int_0^\infty-\frac{w_s}{U_s}\,dy$$

$$\theta_{11}=\int_0^\infty\left(1-\frac{u_s}{U_s}\right)\frac{u_s}{U_s}dy \tag{31}$$

$$\theta_{13}=\int_0^\infty\left(1-\frac{u_s}{U_s}\right)\frac{w_s}{U_s}\,dy$$

$$\theta_{31}=\int_0^\infty-\frac{u_sw_s}{U_s^2}dy$$

$$\theta_{33}=\int_0^\infty-\frac{w_s^2}{U_s^2}dy$$

$$H=\frac{\delta_1}{\theta_{11}}$$

Cross flow angle β and β_w (limiting stream line angle) are obtained by

$$\tan\beta=\frac{w_s}{u_s}\ ;\ y>0$$

$$\tan\beta_w=\frac{\left(\frac{\partial w_s}{\partial y}\right)_w}{\left(\frac{\partial u_s}{\partial y}\right)_w}\ ;\ y=0 \tag{32}$$

Shear stresses on the wall are obtained by

$$\tau_{wx}=\mu\left(\frac{\partial u}{\partial y}\right)_w,\quad \tau_{wz}=\mu\left(\frac{\partial w}{\partial y}\right)_w \tag{32}$$

Therefore stream-wise and cross-wise skin frictions are given by

$$\tau_{ws}=\tau_{wx}\cos\alpha+\tau_{wz}\sin\alpha$$

$$\tau_{wc}=-\tau_{wx}\sin\alpha+\tau_{wz}\cos\alpha \tag{33}$$

Then the angle of limiting stream line becomes

$$\tan\beta_w=\frac{\tau_{wc}}{\tau_{ws}} \tag{33}$$

2.3 Boundary Conditions and Initial Conditions

Three dimensional boundary layer equations are known to be hyperbolic in the surface parallel to the body-surface[16]. Informations are convected along stream lines in the boundary layer and also transported normal to the wall by viscous diffusion. Therefore conditions at a point in the boundary layer depend only on conditions in a wedge-like domain of dependence, extending upstream from the point, bounded by two surfaces normal to the wall which enclose all the stream lines passing through the line of intersection.

In case of ship forms, boundary conditions on the body surface, at the outer edge of the boundary layer and along the plane of symmetry and intitial conditions at the upstream should be specified according to the above "influence principle." Potential-velocity fields are usually obtained in (X,Y,Z) or (X,R,θ) coordinates. When (U_1,U_2,U_3) denote three componen ts of velocity in each direction, external velocity components in x and z direction are given by as follows.[3]

$$U=\frac{\left(1+F_T^2\right)U_1+F_XU_2-F_XF_TU_3}{\sqrt{\left(1+F_T^2\right)\left(1+F_X^2+F_T^2\right)}} \tag{31}$$

$$W=\frac{F_TU_2+U_3}{\left(1+F_T^2\right)} \tag{35}$$

where derivatives in eq. (34) and eq. (35) are defined in eq. (3). The boundary conditions along the plane of symmetry are obtained by solving the plane of symmetry flow. On the other had, measured velocity profiles or estimated ones at the starting point of calculations should be given as initial conditions, or calculations should be preceeded from the stagnation point at the bow. Proper handling of the geometry and coordinate system is very complex [7]. Therefore reasonably estimated initial conditions are enough in case of the after-body calculation, since effects of initial conditions are decaying in the downstream. If necessary, smaller step size might be helpful at the biginning.

2.4 Numerical Procedure

In order to solve the boundary layer equations, derivatives are represented by finite-difference forms. But the influence principle should be obeyed. In the original program of Chang and Patel [3] has adopted the well known Crank-Nicolson type finite-difference scheme. But the ability of this scheme is quite limited to the uni-directional cross flow frofile. Even though the Crank-Nicolson type scheme can handle the weakly sign-changing cross flow, the numerical results show unstable overshooting velocity profiles.[13] Therefore different scheme (scheme 2) is used for the region where the sign of the cross flow is changing [7] [8]. Scheme 2 is selected in this study when the potential velocity W is adverse to the marching direction. Theses sehemes are represented in Fig. 2.

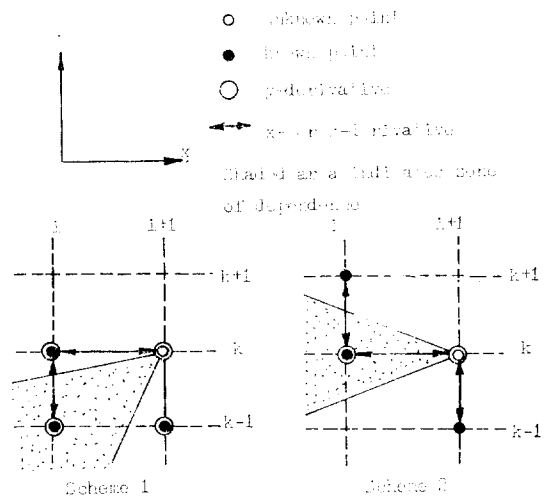

Fig. 2 Finite difference schemes

Details of both numerical schemes will not be represented here(refer to [3] and[7]). The boundary layer equations are originally coupled non-linear equations. Linearizing and decoupling will be accomplished by

$$Q^2=Q\cdot Q$$

$$Q_1Q_2=Q_1\cdot Q_2$$

where Q, Q_1 and Q_2 denote dependent variables and the overbar represents an assumed value or a value

of the previous iteration. Then momentum equations become a simple algebraic equations, which can be easily solved by Thomas alogrism.

$$A_j(Q)Q_{j-1}+B_j(Q)Q_j+C_j(Q)Q_{j+1}=D_j(Q) \quad (36)$$

Both finite-difference schemes are implicit in y-direction. Therefore all the values at points in y-direction should be solved simultaneously. After momentum equations are solved, v will be obtained from the continuity equation in the explicit form. The procedure will be repeated until satisfactory convergence is obtained.

The step size Δz is determined according to the external flow, but stream wise step size Δx is taken to be proportional to the boundary layer thickness and to satisfy the Courant-Friedrichs-Levy condition that

$$\frac{\Delta x}{\Delta z}<\left|\frac{u}{w}\right| \quad (37)$$

For the flow with a strong adverse pressure-gradient, the smaller step size may be taken. The grid spacing in y-direction is non-uniform, since velocities across the boundary layer change rapidly near the wall. The grid points are distributed by

$$y_{j+1}=\delta_{\max}\left[C\frac{j}{n}+(1-C)\left(\frac{j}{n}\right)^2\right], \quad j=1,2,\cdots n \quad (38)$$

in case of laminar flow, where $\delta_{\max}$ is the local upper limit of integration satisfying the condition

$$\left|\sqrt{\frac{u^2+w^2}{U^2+W^2}}-1.0\right|\leq 0.0005 \quad (39)$$

For the turbulent flow,

$$y_{j+1}=y_2\frac{\gamma^j-1}{\gamma-1}, \quad \gamma>1, \quad j=2,3,\cdots\cdots n \quad (40)$$

is adopted, where γ is determined such that the condition

$$\frac{y_2 u_\tau}{\nu}<4.0 \quad (41)$$

is satisfied. The first grid point should be in the laminar sublayer to give the reasonable shear stress at the wall. Maximum number of grid points n is limitted by computer capacity, but 30 to 40 is reasonable for usual cases.

The boundary layer usually grows in thickness along downstream. When eq. (39) is not satisfied, several grid points are added until new $\delta_{\max}$ is 15% more than the original one. When the number of grid points become maximum allowed, a new grid pattern is arranged according to eq. (38) or eq. (40). The velocity components at new grid points are obtained from the values at old grid points by using four-points Lagrangian interpolation.

III. Applications to ship forms

The capability of the above method with Crank-Nicolson type numerical scheme are demonstrated by Chang and Patel [3] in case of mathematical ship-like bodies and by Choi [18] for boundary layer flows over an axisymmetric body with incident angle. The auther also has rechecked the program through the preliminary study [13]. The main purpose of this paper is to compare calculated results with experimental data of real ships with modified numerical schemes.

3.1 SSPA Model 720

This is one of the SSPA cargo linear series. Its main dimensions are

$L=2.0$m $\quad T=0.118$m

$B=0.283$m $\quad C_B=0.675$m

The body plan of the model is represented in Fig. 3 with 3 stream lines, which are selected for the comparison with calculated results. The reason of it is as follows according to Lars Larsson [20]. Line A is in the vertical plane of symmetry. The boundary layer along line A exhibits a peculiar development, since the thickness decreases towards the stern. This is due to a very large divergence of the flow in this region. By selecting this line the ability to compute the divergence and its effect is to be tested. Since line B is highly curved, large cross-flows therefore occur. On the other hand the line never enter the region where boundary layer becomes thick. It is good for the test of the three dimensional first order boundary layer method. The boundary layer along C grows very thick at the stern, therefore it may be adequate to check the superiority of the higher order method.

The calculations are carried out at a Reynolds number, based on the model length, equal to 5.0×10^6, starting at $2x/L=-0.6$. Calculated potential-

SSPA MODEL 720

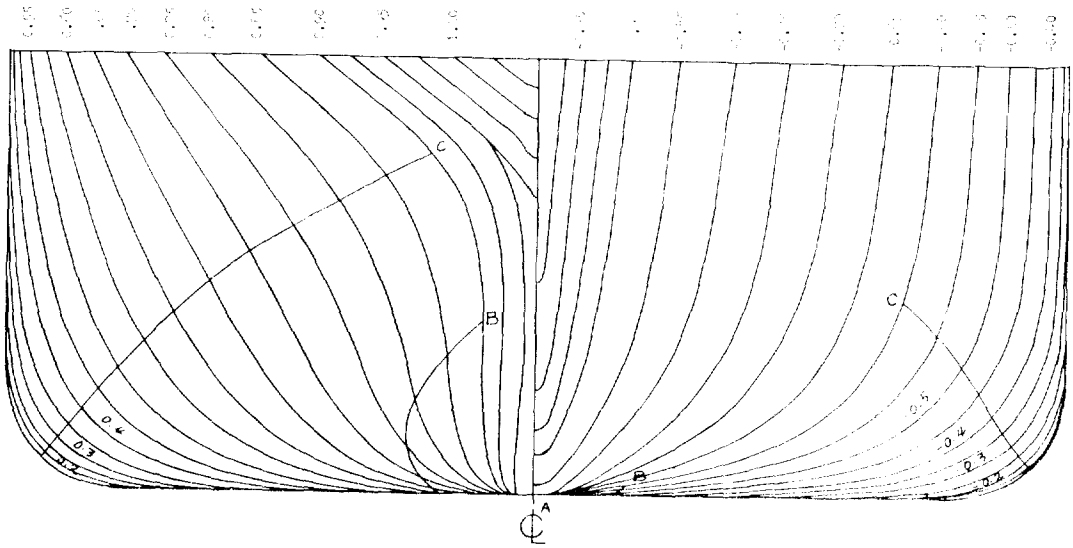

Fig. 3 Body plan of SSPA Model 720

flow velocities by using Hess and Smith method after blockage corrections and a simple computer program to generate the initial velocity profiles are available. Polar coordinate system are adopted. 18 equal-spaced grids in θ direction are adopted and 30~35 grid points in y direction are taken.

Calculations proceeded from the keel line to the water line. Therefore the keel line is taken as the plane of symmetry.

Variations of momentum thickness, θ_{11}, limiting cross flow angle β_w, shape factor H and skin friction coefficients C_f along lines A, B and C are represented in Fig. 4 to Fig. 7 and compared with experimental data. Generally speaking calculated results

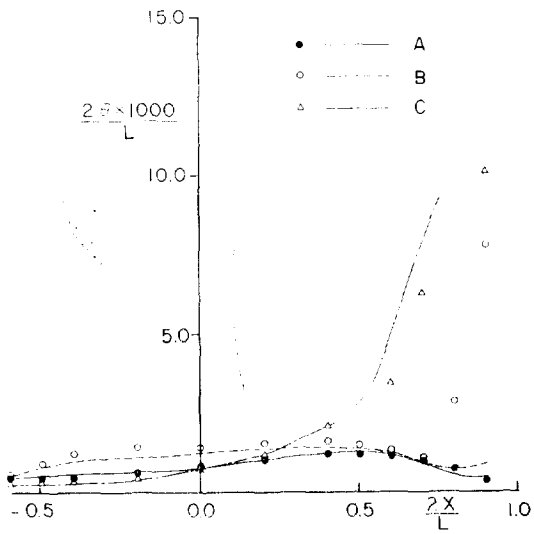

Fig. 4 Momentum thickness along lineA, B and C

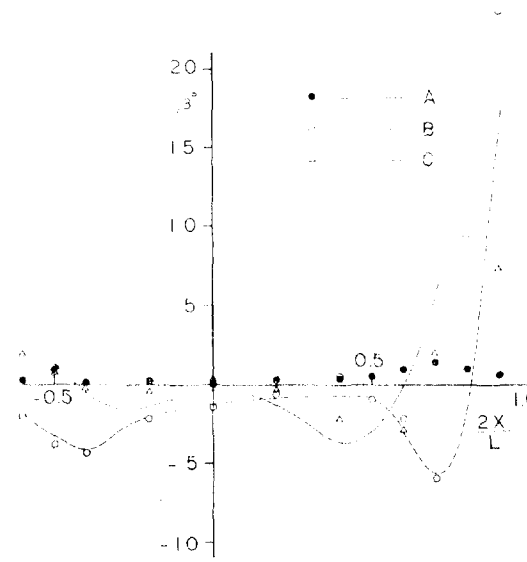

Fig. 5 Cross flow angle along line A,B and C

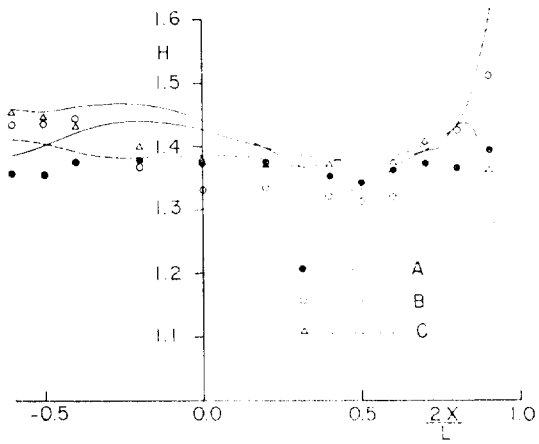

Fig. 6 Shape factor along line A,B and C

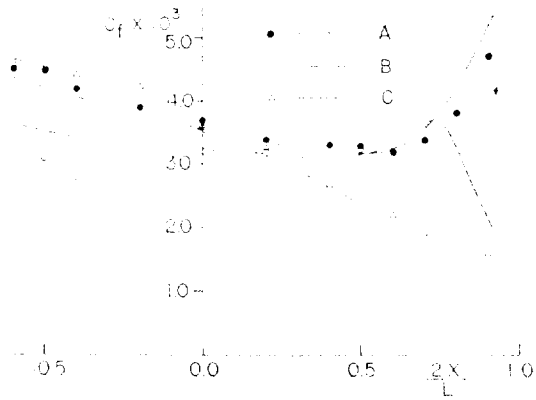

Fig. 7 Skin friction coefficient along line A,B and C

show good agreement with experiments qualitatively up to $2x/L=0.7$. Predictions along line A is quite successful, but calculation along C is failed after that. Girth-wise distributions of θ_{11}, H and β_w at stations $2x/L=0.5$, 0.7 and 0.9 are represented in Fig. 8-Fig. 10. Actually the flow down the station $2x/L=0.5$ are considered to be in the region of the stern boundary layer. Predicted θ_{11}, H and β_w at $2x/L=0.5$ are qualitatively in good agreement with experiments in Fig. 8, but they show an unstable behavior between the line C and the water line at the station $2x/L=0.7$ (Fig. 9) The results at $2x/L=0.9$ are not obtained according to numerical separation, except the keel line (Fig. 10). The polar coordinate system adopted in this study seems to be inadequate for handling the stern geometry in this case.

Stream-wise and cross-wise velocity profiles along line A, B and C at $2x/L=0.5$, 0.7 and 0.9 are represented from Fig. 11 to Fig. 15. As the case of integral parameters, except at $2x/L=0.9$, velocity profiles show reasonable trends even in cross flows. Further improvement of the numerical method should be developed for the stern boundary layer. At the beginning of calculation ($2x/L=-0.6$-0.0) the value of W is negative. Therefore scheme 2 should be adopted. When the scheme 1 is adopted in this region, over shootings are appeared in the stream-wise velocity profile. These overshootings generate the numerical separations.

Fig. 8 Integral parameters at 2X/L=0.5

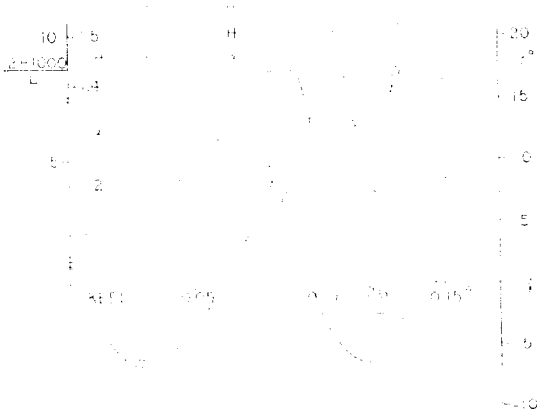

Fig. 9 Integral parameters at 2X/L=0.7

Fig. 10 Integral parameters at 2X/L=0.9

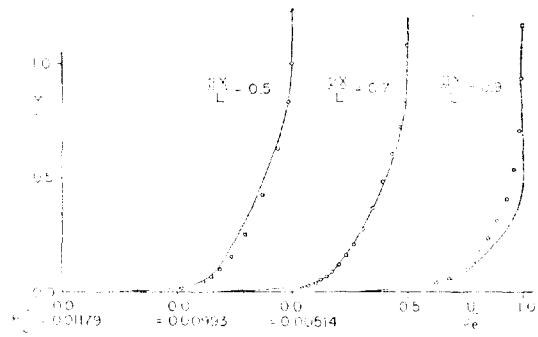

Fig. 11 Stream-wise velocity profiles along line A (plane of symmetry flow)

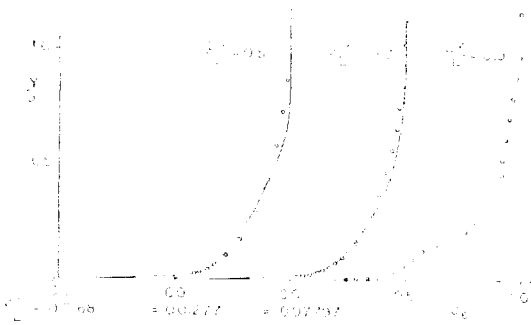

Fig. 12 Stream-wise velocity profiles along line B

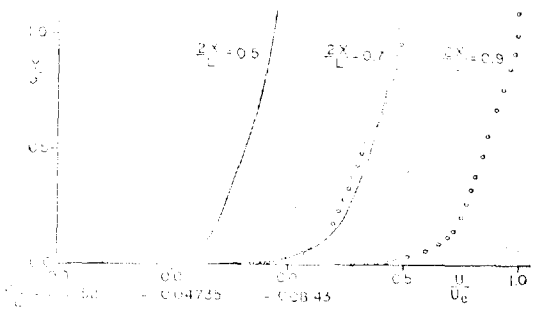

Fig. 13 Stream-wise velocity profiles along line C

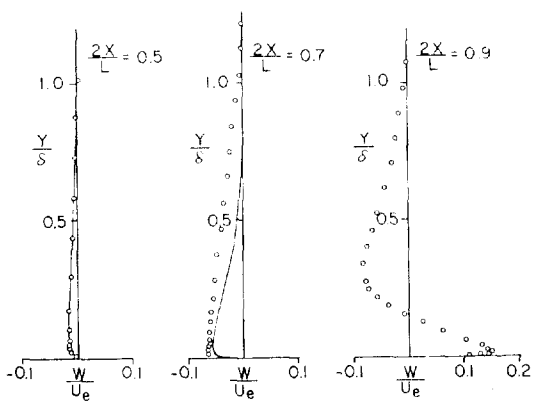

Fig. 14 Cross-flow velocity profiles along line B

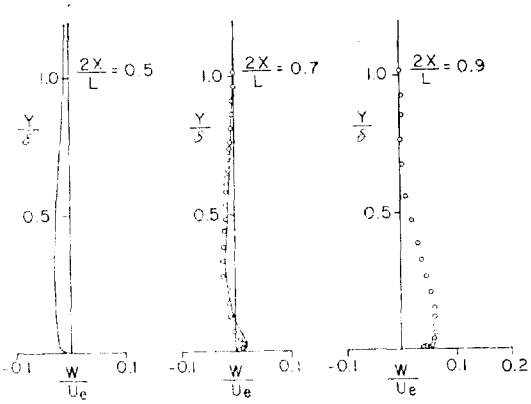

Fig. 15 Cross-flow velocity profiles along line C

3.2 HSVA Tanker Model

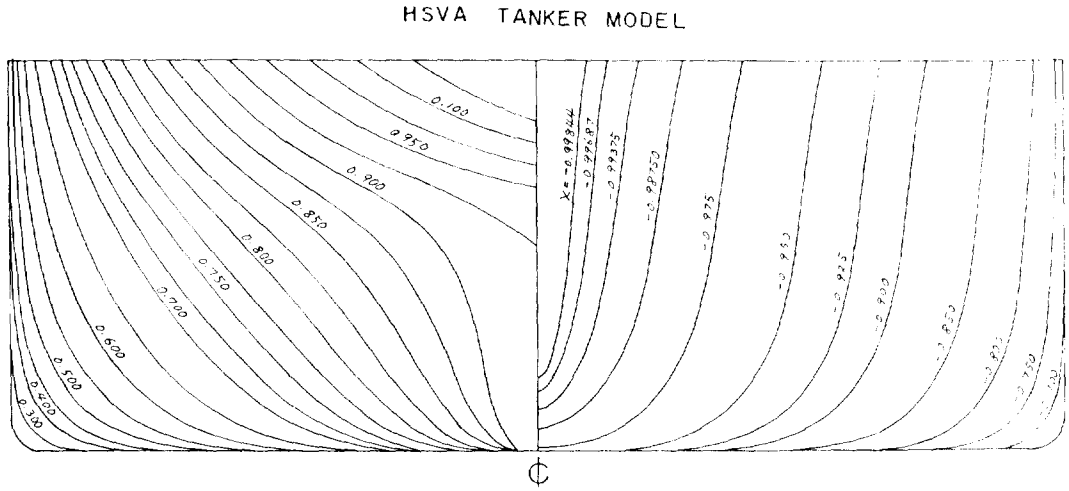

Fig. 16 Body plan of HSVA Tanker model

This tanker model is characterized by a very high block coefficients, $C_B=0.85$, and long parallel middle body. Therefore large three-dimensionality near the stern region and small radius of curvature near the bilge make it difficult to calculate the boundary layer developments. In Hoffmann's measurements L was 2.664m. Calculation is started from $2x/L=-0.790$ with $R_L=6.6\times10^6$. The step size in x-directions and the number of grid point are taken as same as before. Girth-wise distribution of integral parameters at $2x/L=-0.744$, 0.291, 0.502 and 0.884 are represented in Fig. 17-Fig. 20. But calculated results at $2x/L=0.884$ are not shown according to early separation before this station. The results at $2x/L=-0.744$, which is a little down stream from the start-point, are shown in Fig. 17. The θ_{11} is nicely predicted, and H and β_w are good in quality. There are appeared some deviations of H and β_w near the water line and the bilge. At $2x/L=0.291$(Fig. 18), which is a little down stream from the midship section, calculated results also show good agreements with measurements. At this station the flow is nearly two dimensional except the bilge region. The station $2x/L=0.502$, which is amid of the midship section and stern. The trend is still good, but considerable discrepancies are there around the bilge keel and the water line. Careful calculations are required to avoid these unstable results between the bilge and the water line. Calculations cannot reach the station $2x/L=0.884$, show numerical separation around the

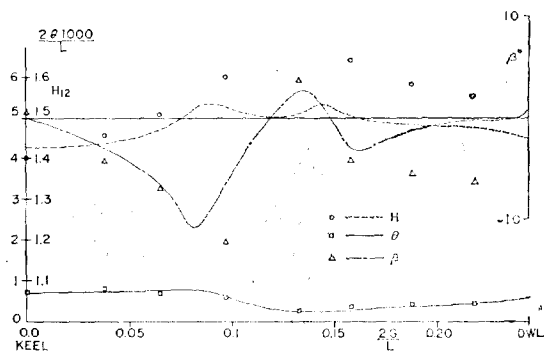

Fig. 17 Integral parameters at 2X/L=−0.744

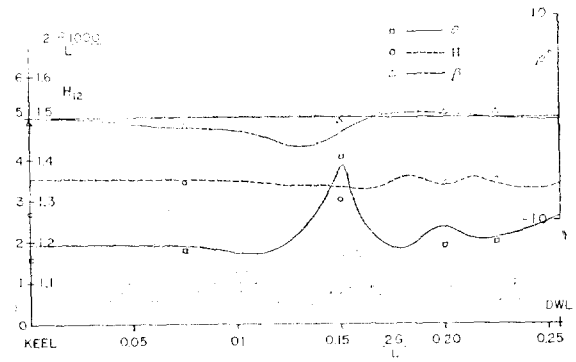

Fig. 18 Integral parameters at 2X/L=0.291

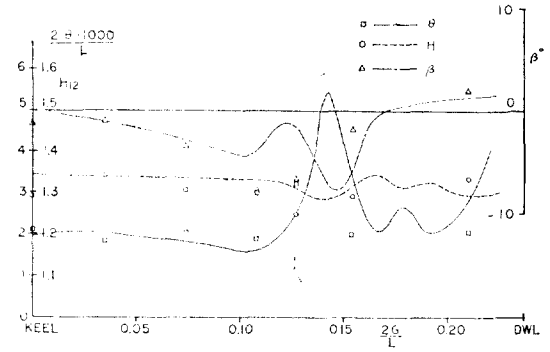

Fig. 19 Integral parameters at 2X/L=0.502

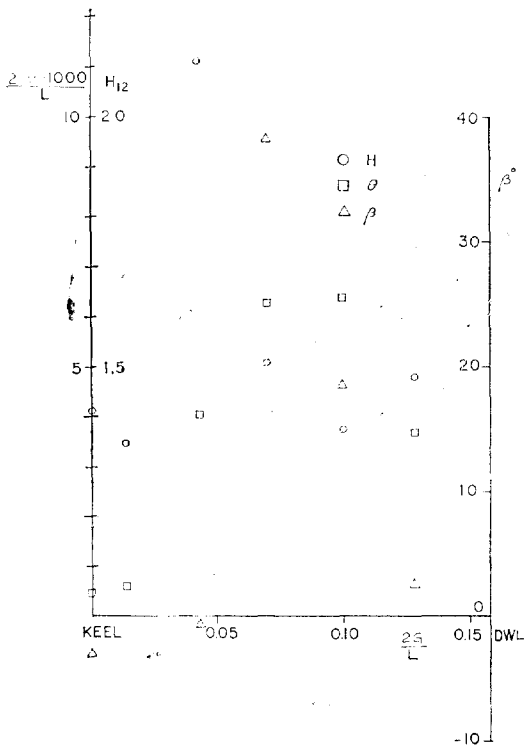

Fig. 20 Integral parameters at 2X/L=0.884

station $2x/L=0.80$. Therefore results cannot be compared with measurements at this station.

IV. Conclusion

Theoretical predictions of the boundary layer development on the typical ship from, SSPA cargo liner and HSVA tanker model, are tried by using the available computer program with modified numerical schemes. The method belongs to the three dimensional thin boundary layer theory. Predicted results generally show good agreement with measurements qualitatively, except in the stern. During the calculation, coordinate systems adopted for the potential-flows calculation, the boundary layer calculation, and the representation of messurements are different each other. Therefore there seems to be considerable uncertainties in the results during interpolating numerical values. But the author conclude that the method adopted here is very promising to predict the boundary layer flow on the ship form with some more developments.

To analize the thick stern boundary layer, lots of theoretical and experimental efforts should be concentrated, i.e, the effect of higher order terms, the behavior of Reynslds stresses, the interaction between the boundary layer and the external flow, free surface effects, etc.

Before closing the paper, the author wishes to show his deep appreciation to Dr. Chang and Prof. Patel for their computer program, which was available through Dr. Choi's thesis. He also appreciates to Dr. Larsson for his kind submittng materials of ITTC-SSPA workshop. He thainks to Mr. Lee, Young-Gill, and Mr. Hyun Bum-Soo for their great assistances to prepare this paper.

References

[1] L. Landweber and V.C. Patel, "Ship Boundary Layers", Annual Review of Fluid Mechanics, Vol. 11, 1979.

[2] T. Cebeci, et al, "A General Method for Calculating Three Dimensional Incompressible Laminar and Turbulent Boundary Layers. Ⅲ. Three Dimensional Flows in Curvilinear Orthgonal Coordinates", Douglas Aircraft Co. Rep. MDC-J6867, 1975.

[3] K.C. Chang and V.C. Patel, "Calculations of Three Dimensional Boundary Layers on Ship Forms", IIHR Rep. 178, The Univ. of Iowa, 1975.

[4] T. Cebeci and K.C. Chang, "A General Method for Calculating Three-Dimensional Laminar and Turbulent Boundarylayer on Ship Hulls, 1.

Coordinates System, Numerical Method, and Preliminary Results", Rept. of Mech. Eng., Calf. St. Univ. in Long Beach, 1977.

[5] S. Soejima and R. Yamazaki, "Calculations of Three-Dimensional Boundary Layers on Ship Hull Forms," Trans. of the West-Japan Soc. of Naval Architecture, No. 55, March 1978.

[6] T. Cebeci, K. Kaups, and A. Moser, "A General Method for Calculating Three-Dimensional Laminar and Turbulent Boundary Layer on Ship Hulls", 12th Symp. on Naval Hydrodynamics, or Ocean Engineering Vol. 7, No. 2, 1980.

[7] M. Hoekstra, "Boundary Layer Flow Past a Bulbous Ship-Bow at Vanishing Froude Number," Int. Symp. of Ship. Viscous Resistance, Goteborg, Sweden, 1978.

[8] H.C. Raven, "Calculation of the Boundary Layer Flow Around Three Ship After-Bodies, I.S.P. Feb., 1980.

[9] A.M. Abdelmeguid, et al, "A Method of Predicting Three-Dimensional Turbulent Boundary Layer around Ships' Hulls", Int. Symp. of Ship Viscous Resistance, Goteborg, Sweden, 1978.

[10] K. Murauka, "Calculation of Thick Boundary Layer and Wake of Ships by a Partially Parabolic Method", 13th Symp. on Naval Hydrodynamics, Tokyo, 1980.

[11] L. Larsson, "Boundary Layers of Ships. Part Ⅲ: An Experimental Investigation of the Turbulent Boundary Layer on a Ship Model", SSPA Rept. No. 46, Sept. 1974.

[12] H.P. Hoffmann, "Untersuchung der 3-Dimensionalen, Turbulenten Grenzschicht an einem Schiffsdoppelmodell im Windkanal", Institut fur Schiffbau der Universitat Hamburg, Bericht, Nr. 343, 1976.

[13] S.H. Kang, "Calculation of Three-Dimensional Boundary Layer on Ship Forms", Korea Inst. of Machinery and Metals (Ship Ressearch Station) Rept. Uce 72-113 A.D., 1981.

[14] Hess and A.M.O. Smith, "Calculation of Potential Flow about Arbitrary Three-Dimensional Bodies", Douglas Aircraft Co. Rept. No. E.S. 40662, 1962.

[15] T. Miloh and V.C. Patel, "Orthogonal Coordinates System for Three-Dimensional Boundary Layers, with Particular Reference to Ship Forms", JSR Sep. 1973.

[16] J. Nash and V.C. Patel, *Three-Dimensional Turbulent Boundary Layers*, SBC Technical Books, 1972.

[17] T. Cebeci and A.M.O. Smith, "A Finite-Difference Solution of the Incompressible Turbulent Boundary Layer Equations by an Eddy-Viscosity Concepts, "Proc. AFOSR-IFP Stanford Conf., 1968.

[18] D.H. Choi, "Three-Dimensional Boundary Layers on Bodies of Revolution at Incidence", Ph. D. Thesis, The Univ. of Iowa, 1978.

[19] K.K. Chen and N.A. Thyson, "Extensions of Emmon's Spot Theory to Flows on Blunt Bodies, "J. of AIAA, 9, 821, 1971.

[20] L. Larsson, SSPA-ITTC Workshop on Ship Boundary Layers, Input-Output Definition for Case No. 1, the SSPA Model 720.